Cleavage of Double-Crossover Molecules by T4 Endonuclease VII†

Tsu-Ju Fu,‡ Börries Kemper,§ and Nadrian C. Seeman*,‡

Institute of Genetics, University of Köln, 5000 Köln 41, Germany, and Department of Chemistry, New York University, New York, New York 10003

Received November 23, 1993; Revised Manuscript Received January 25, 1994®

ABSTRACT: DNA double-crossover molecules containing two Holliday junctions have been prepared and treated with endonuclease VII, the resolvase from bacteriophage T4. One molecule contains antiparallel double-helical domains, and the other molecule contains parallel domains. The parallel double-crossover model system has been made tractable by closing the free ends of the molecule, to convert it to a catenane. The products resulting from the two substrates differ substantially. The molecule containing antiparallel helical domains is cleaved three nucleotides 3′ to the crossover points, in a fashion similar to single Holliday junction analogs. The molecule containing parallel helical domains is cleaved, but the major points of scission are five nucleotides 5′ to a branch point on the crossover strands and six nucleotides 3′ to the same branch point on the non-crossover strands. The major sites of scission reflect features of molecular symmetry in each case, suggesting that the resolvase recognizes structural features. The cleavage results suggest that the antiparallel structure is the natural substrate, if the Holliday junction is unconstrained within the cell. It is straightforward to reconcile antiparallel Holliday junctions with the conventional parallel paradigm of recombination. Nevertheless, the cleavage of the parallel molecule shows that a parallel substrate could also be cleaved symmetrically by endonuclease VII (but with different products) if the molecule were constrained to assume that conformation within the cell.

Recombination is a process that promotes genetic diversity within all living species. The basic feature of recombination is the interaction of two pieces of DNA to yield new genetic material that may physically incorporate segments of both interacting molecules. The resulting DNA may contain insertions, deletions, changes of sequence, rearrangements, or exchanges of flanking markers. The Holliday (1964) junction is a central intermediate in recombination, known to participate in site-specific recombination (Hsu & Landy, 1984; Hoess *et al.*, 1987; Kitts & Nash, 1987; Nunes-Duby *et al.*, 1987) and thought to be involved in homologous recombination as well (Dressler & Potter, 1982). This is a four-stranded molecule containing a branch point surrounded by four double-helical arms, as shown at the top left of Figure 1. In naturally occurring systems, the sequence flanking the branch point of the Holliday junction is twofold symmetric (homologous), enabling the branch point to migrate (Kim *et al.*, 1972; Thompson *et al.*, 1976; Panyutin & Hsieh, 1992; Johnson & Symington, 1993).

For the past decade, Holliday junctions have been modeled by a non-migrating analog system, 4-arm immobile junctions (Seeman, 1982; Kallenbach *et al.*, 1983) that lack twofold sequence symmetry. The term "immobile" here refers to the inability of these molecule to undergo branch migration. Several laboratories have characterized the qualitative structure of immobile junctions in solution [for reviews, see Lilley and Clegg (1993) and Seeman and Kallenbach (1994)]. The key structural feature noted for the 4-arm immobile branched junction is that its four arms assort themselves to form two helical stacking domains (Figure 1, center) (Cooper & Hagerman, 1987, 1989; Churchill *et al.*, 1988; Chen *et al.*, 1988; Duckett *et al.*, 1988). Thus, two of the strands (termed the "helical" strands) have a structure similar to that of ordinary double-helical DNA, and the other two strands (termed the "crossover" strands) form the bridge between the two domains. In principle, the 5′→3′ directions of the helical strands can be antiparallel (Figure 1, center), parallel (Figure 1, right), or anywhere in between. The designations "parallel" and "antiparallel" refer to the orientations of the helical strands. The antiparallel structure is favored over the parallel structure (Cooper & Hagerman, 1987, 1989; Duckett *et al.*, 1988), although the preference is not striking (Lu *et al.*, 1991). Cooper & Hagerman (1989) have presented data that the angle differs from exact antiparallelism by about 60°, a figure also suggested by Murchie *et al.* (1989). Eis & Millar (1993) have shown that there is a large dispersion about this apparently favored angle.

The genetic derivation of the Holliday (1964) junction has led to the use of parallel junctions in most modeling of recombination events. The involvement of the Holliday junction in recombination is illustrated with parallel helical domains in Figure 2. Six stages are shown, with five steps between them. First is the formation of the junction, which generally requires the involvement of protein cofactors [reviewed in West (1992)]. This is followed by branch migration, a process that can be spontaneous (Kim *et al.*, 1972; Thompson *et al.*, 1976; Panyutin & Hsieh, 1992; Johnson & Symington, 1993) or catalyzed by proteins (Tsavena *et al.*, 1992; Lloyd & Sharples, 1993). Little is known about the third, optional, step, crossover isomerization, in which the crossover strands and the helical strands exchange roles. In the fourth step, the junction is cleaved to linear duplex by a resolvase, followed by ligation to seal the nicks introduced by the resolution process.

Given the antiparallel structure of Holliday junction analogs in solution, it is important to ask whether the parallel or antiparallel structure of the Holliday junction actually participates in reactions that occur in recombination. Here,

† This research has been supported by grant GM-29554 from the National Institutes of Health and by support from the Deutsche Forschungsgemeinschaft through SFB 74.

* To whom correspondence should be addressed.
‡ New York University.
§ University of Köln.

® Abstract published in *Advance ACS Abstracts,* March 15, 1994.

0006-2960/94/0433-3896$04.50/0

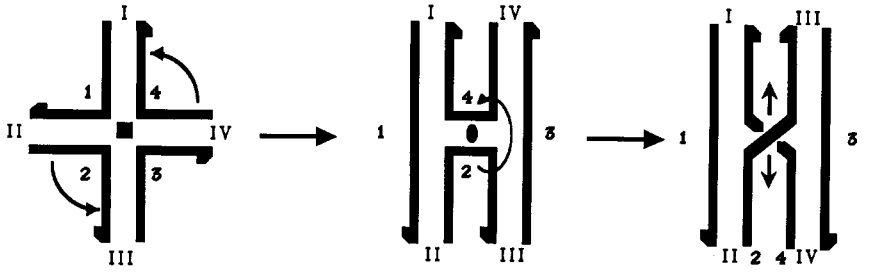

FIGURE 1: Conformers of the Holliday structure. Each strand is numbered with Arabic numerals, and each arm is labeled with Roman numerals. The 3′ ends of strands are indicated by half-arrowheads; double-helical regions, by parallel lines. On the left is the structure implicit from the sequence, whose possible fourfold symmetry is indicated by the square in the center of the figure. If the arms stack as indicated by the curved arrows, one obtains the antiparallel structure indicated at the center. Note that this structure is twofold symmetric, as indicated by the lens-shaped object. Note that the helical (straight) strands are antiparallel. This structure may be transformed into a parallel structure by rotating the domain at the bottom. The parallel structure is shown at the right. Note that its helical strands are parallel and that the twofold axis lies in the plane of the page and is indicated by the double-headed arrows.

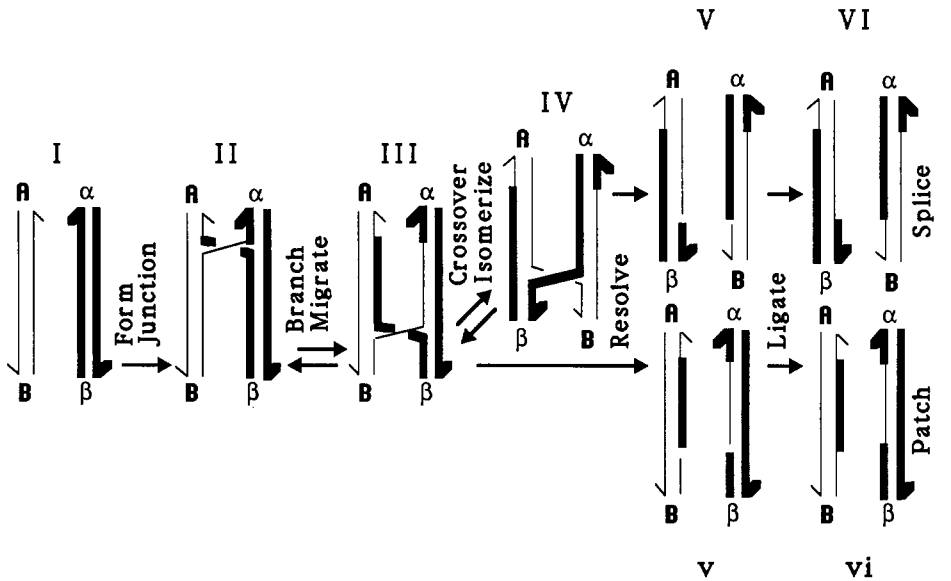

FIGURE 2: Formation and resolution of the Holliday structure in genetic recombination. The process is shown proceeding from the left to the right. Each of the possible stages is labeled with a capital or small Roman numeral. In the first stage, I, two homologous double helices of DNA align with each other. The two strands of each duplex are indicated by the two pairs of lines terminated by half arrows, which indicate the 3′ ends of the strands. Strands are distinguished by their thickness. Each of these two homologous regions carries a flanking marker, A and B in the strands on the left, and α and β on the right. After the first step, the homologous pairs have formed a Holliday intermediate, II, by exchanging strands. Note that the two crossover strands are composite strands with both a thick and a thin portion, formed through any of a number of possibilities. The parallel representation of the Holliday junction is shown. The homologous twofold sequence symmetry of this structure permits it to undergo the iterative isomerization process, branch migration; movement in the direction indicated results in structure III. The Holliday intermediate may or may not undergo the crossover isomerization process to produce structure IV, in which the crossover and non-crossover strands are switched. Note that this process only has meaning if the Holliday intermediate is twofold, rather than fourfold, symmetric. If crossover isomerization occurs an odd number of times, resolution by cleavage of the crossover strands yields structure V, but structure v results if crossover isomerization occurs an even number of times (including 0) before cleavage. Ligation of v generates a patch recombinant, vi; this is a pair of linear duplex DNA molecules containing heteroduplex DNA because of branch migration but retaining the same flanking markers. Ligation of VI yields splice recombinant molecules that have exchanged flanking markers.

we address this question with regard to the fourth step, the resolution of the junction into two duplex molecules. A number of enzymes have been identified that perform this operation (West, 1992), but the best studied molecule with this activity is endonuclease VII (endo VII), the product of *gene 49* of bacteriophage T4 (Kemper & Janz, 1976; Kemper & Brown, 1976). The protein has been characterized as a dimer of subunit molecular weight ca. 18 000 (Kosak & Kemper, 1990). It has been shown to cleave partially mobile Holliday junctions (Mizuuchi *et al.*, 1982), cruciforms extruded from negatively supercoiled plasmids (Lilley & Kemper, 1984), 3-arm junctions (Jensch & Kemper, 1986), and heteroduplex loops (Kleff & Kemper, 1988). In previous work, we (Mueller *et al.*, 1988) and others (Duckett *et al.*, 1988) have shown that this enzyme cleaves the crossover strands of Holliday junctions, and we have demonstrated that the enzyme has a requirement for at least nine nucleotide pairs on an arm to show resolvase activity (Mueller *et al.*, 1990). Kemper *et al.*, (1990) have found that the enzyme shows endonucleolytic activity on a variety of unusual DNA structures, in addition to Holliday junctions, and Pottmeyer & Kemper (1992) have shown that the enzyme cleaves by a double-nicking activity.

It is of particular interest to characterize the activity of endo VII with respect to helical domain orientation. In order to answer this question, we initially developed tethered junctions, in which the orientations of the helical domains, as well as the crossover isomers, are under the control of single-stranded oligo-dT tethers that link two arms of the junction (Kimball *et al.*, 1990). For example, the junction at the center of Figure 1 can be constrained to assume the antiparallel structure shown by linking the 3′ end of strand 3 to the 5′ end of strand 1 by a tether consisting of $(dT)_6$; likewise, the junction on the right of Figure 1 can be restricted to the parallel structure presented by linking the 3′ end of strand 4 to the 5′ end of

strand 3 by a tether consisting of $(dT)_9$ (Kimball *et al.*, 1990). Attempts to determine the orientational cleavage preferences of endo VII have revealed that the enzyme cleaves the tethers, particularly in parallel molecules (Mueller, 1991). The inability to determine whether tether cleavage is followed directly by resolution, perhaps without dissociation of the resolvase, makes this system unattractive to use for assaying parallel and antiparallel cleavage by endo VII. Nevertheless, Bhattacharyya *et al.* (1991) have described experiments in which they use endo VII and other resolving enzymes to cleave tethered antiparallel junctions. They find that they can direct the products of the reaction between the two antiparallel alternatives by changing the tethering so as to produce the two antiparallel crossover isomers. Similarly, Lu *et al.* (1991) have used tethered junctions to show that the cleavage products of endonuclease I, a resolvase from bacteriophage T7, differ between parallel and antiparallel structures.

Recently, we have developed double-crossover molecules as a model system to explore the properties of recombination intermediates (Fu & Seeman, 1993). These are molecules that contain two branch points, where the strands cross over between two double-helical domains. There are five isomers of double-crossover molecules (DAE, DAO, DPE, DPOW, and DPON; Figure 3), which have all been constructed. Two of the isomers contain helical domains oriented antiparallel to each other, but the helical domains are parallel in the other three. We have characterized these structures qualitatively by autofootprinting experiments, using hydroxyl radicals generated by $Fe(II)EDTA^{2-}$ (Tullius & Dombroski, 1985; Churchill *et al.*, 1988). Three features of the double-crossover system make it advantageous as a substrate for endo VII: (1) The orientation of the helical domains is determined by the isomer selected. (2) There is no unusual structure present, except for the branch points. (3) In contrast to single junctions (Chen *et al.*, 1988), the crossover isomer is a direct consequence of secondary structure, regardless of the sequence flanking the junction (except for DPE isomers).

We have selected the DAO isomer (Figure 3) to use as an antiparallel double-crossover molecule. This structure self-assembles readily and is well behaved on non-denaturing gels, running as a single band (Fu & Seeman, 1993); unlike the other antiparallel isomer, DAE (see Figure 3), the central portion of DAO contains no cyclic strand whose nick is difficult to seal. Hydroxyl radical autofootprinting reveals that the helix axes of DAO molecules appear to contain coplanar antiparallel helix axes having no bends. Recently, we have reported the construction of symmetric immobile junctions from DAO molecules (Zhang *et al.*, 1993), but we have not used them in the experiments reported here.

Parallel double-crossover molecules present a more complex experimental system. We have found that none of these molecules is well behaved when assayed on non-denaturing gels (Fu & Seeman, 1993): Doublets or multimers are seen frequently in lanes containing parallel isomers. Whereas analysis of the products requires a unique starting material, we have used a variant of the parallel double-crossover molecules to ensure that we have a single species. Using hairpin loops to close the ends of a 4-strand parallel double-crossover molecule converts it into a 2-strand catenated complex. Recently, we have used topological characterization of the catenane derived from a molecule of the DPON isomer (Figure 3), called "DPONCC", to establish the sign of the crossover structure in parallel Holliday junctions (Fu *et al.*, 1994). Here, we use this same catenane to explore the products of endo VII cleavage of parallel crossover molecules.

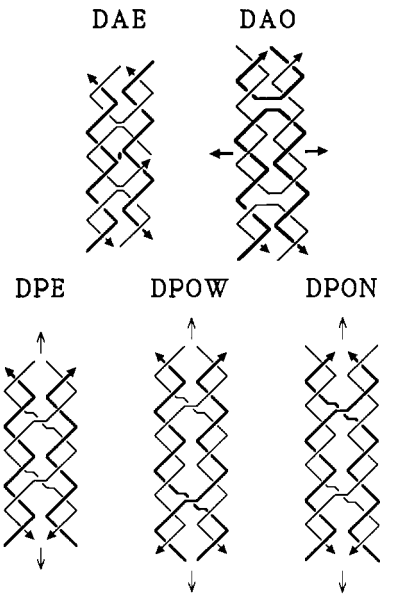

FIGURE 3: Schematic drawings of the five different structural arrangements of double-crossover structures. The structures shown are named by acronyms describing their basic characteristics. All names begin with "D" for double crossover. The second character refers to the relative orientations of their two double-helical domains, "A" for antiparallel and "P" for parallel. The third character refers to the number (modulus 2) of helical half-turns between crossovers, "E" for an even number and "O" for an odd number. A fourth character is needed to describe parallel double-crossover molecules with an odd number of helical half-turns between crossovers. The extra half-turn can correspond to a major (wide) groove separation, designated by "W", or an extra minor (narrow) groove separation, designated by "N". The strands are drawn as zigzag helical structures, where two consecutive, perpendicular lines correspond to a full helical turn for a strand. The arrowheads at the ends of the strands designate their 3′ ends. The structures contain implicit symmetry, which is indicated by conventional markings, a lens-shaped figure (DAE) indicating a potential dyad perpendicular to the plane of the page, and arrows indicating a twofold axis lying in the plane of the page. Note that the dyad in DAE is only approximate, because the central strand contains a nick, which destroys the symmetry. The strands have been drawn as lines of two different thicknesses, as an aid to visualizing the symmetry. In the case of the parallel strands, the dark strands in each structure are related to one another by the twofold axes vertical on the page; similarly, the light strands are symmetrically related to one another. The twofold axis perpendicular to the page relates the two dark helical strands to each other and the two light outer crossover strands to each other. The 5′ end of the central double-crossover strand is related to the 3′ end by the same dyad element. A different convention is used with DAO, where the dark strands are related to the light strands by the dyad axis lying horizontal on the page.

The scheme for this analysis is illustrated in Figure 4. Once we construct the catenated molecule, it can be isolated from a denaturing gel. In contrast to the open complex, it remains a unique species and cannot reequilibrate to form complexes with mixtures of stoichiometries. After renaturation, this molecule is then treated with endo VII. It is necessary to ensure that we are looking at the first scission of the labeled strand. We solve this problem by isolating only full-length, singly nicked, linear molecules from the gel that separates the digestion products. The catenane is deliberately designed to contain sites for cleavage by restriction endonucleases; cleavage at these sites is used to phase the endo VII cleavage sites relative to a fixed position. Restricted fragments are then sized on a gel. We assume that the unlabeled strands are not cleaved by endo VII in a way that permits re-arrangements before a detectable second cleavage on the labeled strands. We find that both parallel and antiparallel molecules are cleaved by endo VII. However, the cleavage pattern of antiparallel molecules matches that of untethered single

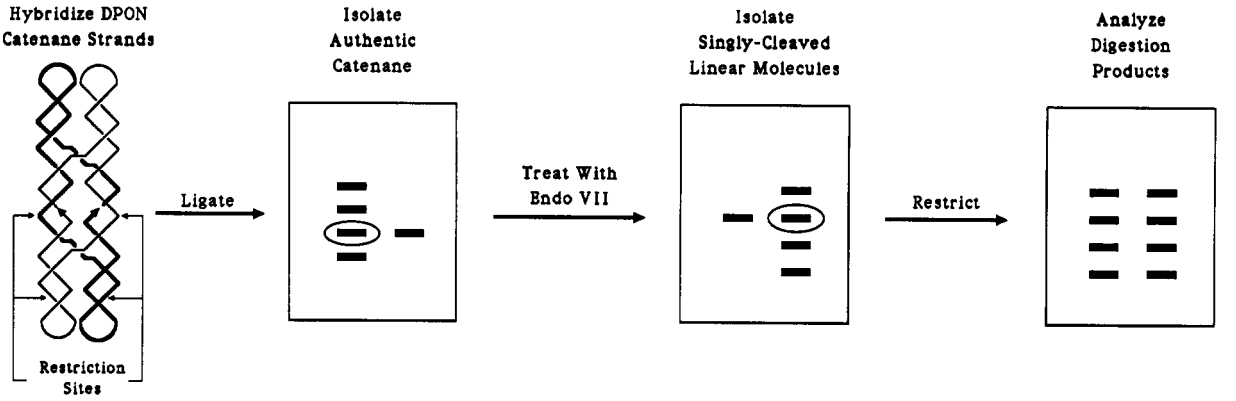

FIGURE 4: Analytical scheme for endo VII cleavage of parallel double crossover molecules. In the first step, the two strands that form the catenane DPONCC are hybridized and then ligated. The two strands are drawn as lines of different thicknesses. Radioactive labeling occurs before hybridization; only one of the two strands contains a label in any given experiment. Authentic catenane is then isolated from a denaturing gel. This ensures proper stoichiometry and eliminates possible reequilibration to other structures. The catenane (labeled in one strand or the other) is then treated with endo VII. Singly nicked 80-mer linear molecules are then isolated. The site of endo VII scission is determined by restricting the labeled strand with a restriction enzyme to phase the position.

Holliday junctions more closely than that of parallel molecules.

MATERIALS AND METHODS

Design of the Substrate. The DAO molecule used is identical to the DAO molecule designed and characterized previously (Fu & Seeman, 1993). DPONCC is based on the DPON molecule characterized previously, but several changes have been incorporated into it: (1) Hairpin loops have been added to the ends of all stems. (2) The arms outside the central region have been extended so that the cyclic strands are each 80 nucleotides long, partly to facilitate topological characterization reported elsewhere (Fu *et al.*, 1994). (3) Restriction sites have been added in the central region and on two of the distal arms. The additional bases have been added, insofar as possible, to minimize sequence symmetry (Seeman, 1982, 1990). The nicks have been placed in the central region at loci that appear on the basis of model building (Seeman, 1988) to be accessible to DNA ligase. The sequence and structural features of DPONCC are shown in the central portion of Figure 5.

Synthesis and Purification of DNA. All DNA molecules used in this study are synthesized on an Applied Biosystems 380B automatic DNA synthesizer, removed from the support and deprotected using routine phosphoramidite procedures (Caruthers, 1985). All strands greater than 30 nucleotides in length are purified by polyacrylamide gel electrophoresis. Shorter strands are purified by preparative HPLC on a DuPont Zorbax Bio Series oligonucleotide column at room temperature, using a gradient of NaCl in a solvent system containing 20% acetonitrile and 80% 0.02 M sodium phosphate. Fractions from the major peak are collected, desalted, and evaporated to dryness.

Formation of Double-Crossover Molecules. The antiparallel double-crossover molecule, DAO, composed of four individual strands, contains a single strand radioactively labeled on the 5′ end. This radioactive strand is then mixed with a 20-fold excess of the other three strands, and the mixture is heated to 90 °C for 5 min and cooled slowly. We have determined by means of gel electrophoresis under native conditions (Fu & Seeman, 1993) that each labeled strand participates only in a 4-strand complex.

The two strands of the parallel catenated double-crossover molecule, DPONCC, are labeled in separate experiments on their 5′ ends. They are mixed with the other strand, heated to 90 °C for 5 min, and cooled slowly. They are then ligated with T4 DNA ligase overnight at 8 °C, and the catenane is purified from a 6% denaturing polyacrylamide gel.

Hydroxyl Radical Analysis of DPONCC. Individual strands of DPONCC are radioactively labeled and are additionally gel purified from an 8% denaturing polyacrylamide gel. Each of the labeled strands [approximately 10 pmol in 40 mM Tris–acetate (pH 8.5) containing 12.5 mM $MgCl_2$ and 2 mM EDTA (TAEMg)] is annealed to a 4-fold excess of the unlabeled complementary strand; incorporated into catenane, as described above; left untreated as a control; or treated with sequencing reagents (Maxam & Gilbert, 1980) for a sizing ladder. The samples are annealed by heating to 90 °C for 3 min and cooling slowly to 4 °C. Purified catenanes are dissolved in TAEMg. Hydroxyl radical cleavage of the double-strand or DPONCC catenane samples takes place on ice for 2 min (Tullius & Dombroski, 1985), with modifications noted by Churchill *et al.* (1988). The reaction is stopped by addition of thiourea. The 80-mer linear DNA molecules, as the single-hit products of hydroxyl radical cleavage, are isolated from an 8% denaturing polyacrylamide gel, extracted, and ethanol precipitated. These 80-mer linear molecules are then digested with restriction enzyme *Nla*III (catenane labeled on strand 1) or *Taq*I (catenane labeled on strand 2). The samples are further phenol extracted, ethanol precipitated, dried, dissolved in a formamide/dye mixture, and loaded directly onto a 6% or 8% polyacrylamide sequencing gel containing 8.3 M urea and 20% formamide. Autoradiograms are scanned with a Hoefer GS300 densitometer in transmission mode.

Enzymatic Reactions. (A) Kinase Labeling. One microgram of an individual strand of DNA is dissolved in 10 μL of a solution containing 66 mM Tris·HCl, pH 7.6, 1 mM spermidine, 100 mM $MgCl_2$, 15 mM dithiothreitol (DTT), and 0.2 mg/mL nuclease-free bovine serum albumin (BSA) (BRL) and mixed with 1–2 μL of 1.25 mM [γ-^{32}P]ATP (10 μCi/μL) and 30 units of polynucleotide kinase (U.S. Biochemical) for 2 h at 37 °C. The reaction is stopped by phenol extraction and ethanol precipitation of DNA.

(B) Ligations. Ligations are performed in the same buffer as phosphorylations. Two units of T4 polynucleotide ligase (U.S. Biochemical) is added, and the ligation proceeds at 8 °C for 18 h. The reaction is stopped by phenol extraction and ethanol precipitation of DNA. Phosphorylated and ligated fragments are purified from denaturing 8% polyacrylamide gels.

(C) Endonuclease VII Digestions. Endo VII is prepared as described previously (Kosak & Kemper, 1990). For 4-strand DAO complexes, 100 ng of DNA is phosphorylated and ethanol precipitated. The labeled strand is then added to a 20-fold excess of the other three strands in a solution containing 40

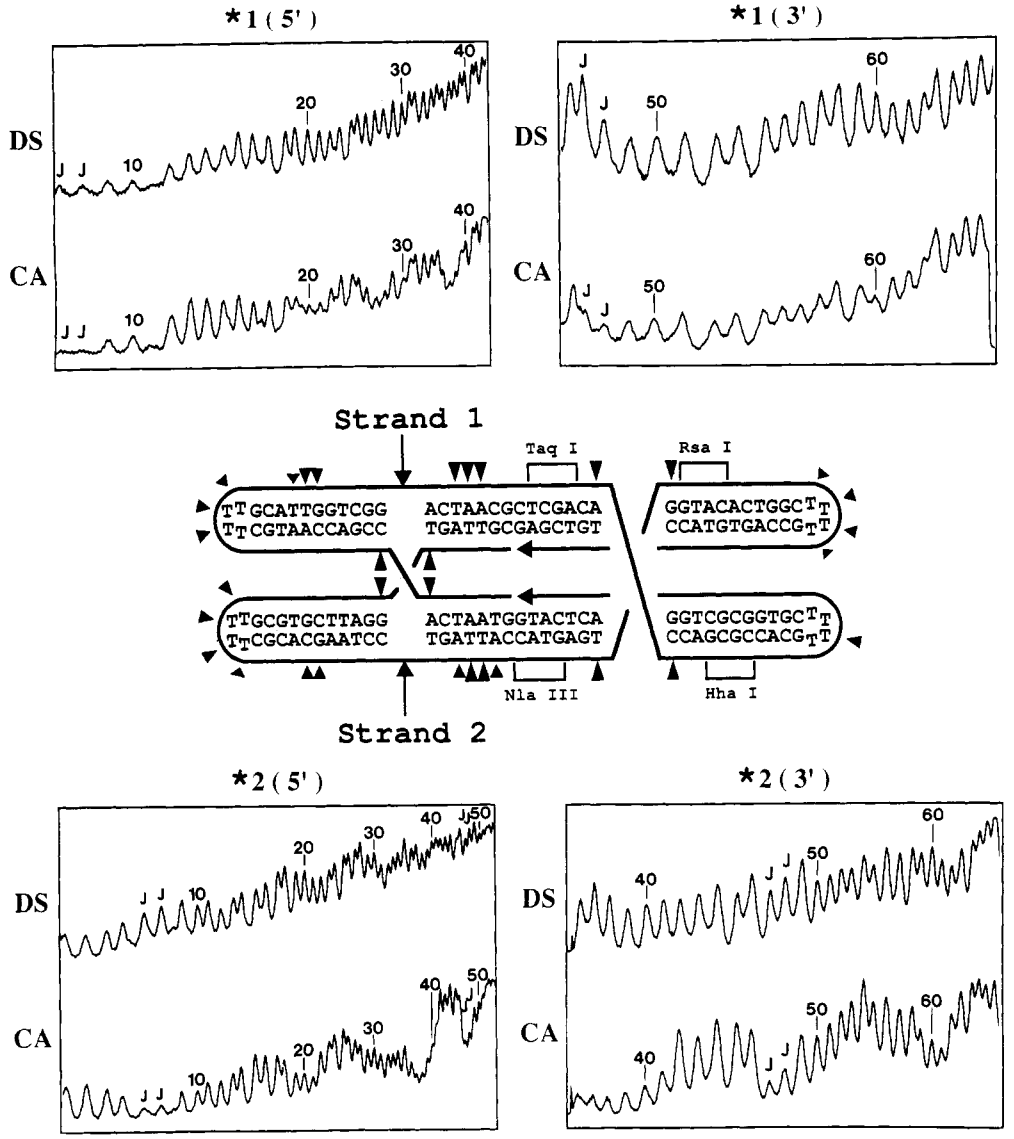

FIGURE 5: Hydroxyl radical autofootprinting of DPONCC. A diagram of DPONCC is shown in the center , indicating the sequence, the restriction sites, the two strands, the sites of crossover, and the ligation site (the 3′ end of the molecule is indicated by an arrowhead). The sites of protection from hydroxyl radical cleavage are indicated by triangles; the size of a triangle is proportional to the amount of protection. The densitometer traces showing the extent of cleavage for each strand are indicated above (strand 1 labeled) and below (strand 2 labeled) the diagram. "DS" refers to the double-stranded control, and "CA" refers to the DPONCC catenane, in each panel. Each point of crossover is indicated by two small J's above the peaks corresponding to the residues. The peaks are numbered from the 5′ end of the molecule. Note that the crossovers and the points 4 nucleotides 3′ to the crossover on the non-crossover strands are protected.

mM Tris–acetate, pH 8.5, 12.5 mM $MgCl_2$, and 2 mM EDTA (TAEMg) in a total volume of 10 μL. The mixture is heated to 90 °C for 5 min and cooled slowly. An equal volume of a solution containing 40 mM Tris–acetate, pH 8.5, 12.5 mM $MgCl_2$, 2 mM EDTA, 200 μg/mL BSA, and 20 mM dithiothreitol is added; 10 μL of this solution is treated with 1 μL of a solution containing endo VII (1000 units/μL) for 1 h at 4 °C. Untreated controls are prepared with enzyme storage buffer substituted for the enzyme.

For DPONCC complexes, approximately 100 ng of catenated DNA is dissolved in 9 μL of TAEMg. The solution is brought to 90 °C for 5 min and allowed to cool slowly. Samples are then brought to a volume of 18 μL in a solution containing 40 mM Tris–acetate, pH 8.5, 12.5 mM $MgCl_2$, 2 mM EDTA, 10 mM β-mercaptoethanol, and 100 mg/mL BSA. This solution is treated at 4 °C with 2 μL of a solution containing endo VII at a concentration of 1000 units/μL. Digestion at higher temperatures has not been attempted for either isomer, in order to avoid possible perturbations of the structures of the branch points. Reactions are stopped after 1 h by phenol extraction and ethanol precipitation. The 80-mer linear DNA products are purified from a denaturing gel and are prepared in the same manner as strands cleaved by hydroxyl radicals, followed by digestion with restriction enzymes. *Hha*I, *Nla*III, and *Taq*I are used to analyze DPONCC labeled on strand 1; *Nla*III, *Rsa*I, and *Taq*I are used to analyze DPONCC labeled on strand 2. Following restriction, the DNA is phenol extracted, ethanol precipitated, and analyzed on a denaturing gel.

(D) Restriction Endonuclease Digestions. Restriction enzymes are purchased from New England Biolabs and used in buffers suggested by the supplier. Digestion is performed at 37 °C for 1 h with 20 units of *Hha*I or 10 units of *Rsa*I or *Nla*III. Digestion with *Taq*I uses 20 units for 1 h at 65 °C. For digestions involving *Taq*I or *Nla*III the complementary catenane strand is added in 10-fold excess to provide the complete restriction site.

Denaturing Polyacrylamide Gel Electrophoresis. These gels contain 8.3 M urea and are run at 55 °C. Gels contain 6–20% acrylamide [19:1, acrylamide:bis(acrylamide)]. Those used to analyze DPONCC molecules contain an additional 20–40% formamide. The running buffer consists of 100 mM

Tris·HCl, pH 8.3, 89 mM boric acid, and 2 mM EDTA (TBE). The sample buffer consists of 10 mM NaOH and 1 mM EDTA containing 0.1% xylene cyanol FF tracking dye. Gels are run on an IBI Model STS 45 electrophoresis unit at 70 W (50 V/cm), constant power, dried onto Whatman 3MM paper, and exposed to X-ray film for up to 15 h. Positions of cleavage are determined by comparing the electrophoretic mobility of products to a 5′-labeled A+G sequencing ladder (Maxam & Gilbert, 1980) of the appropriate molecules.

RESULTS

Hydroxyl Radical Characterization of Substrates. It is key that the substrates used in cleavage experiments be characterized as thoroughly as possible. Previous experiments with hydroxyl radical autofootprinting of structures containing DNA branched junctions have yielded valuable information about the molecules under investigation (Churchill *et al.*, 1988; Chen *et al.*, 1988; Kimball *et al.*, 1990; Lu *et al.*, 1990; Wang *et al.*, 1991; Du *et al.*, 1992; Fu & Seeman, 1993; Zhang *et al.*, 1993). These autofootprinting experiments involve two-part comparisons: (1) Each strand is labeled individually, incorporated as a member of the complex, and then exposed to hydroxyl radicals. (2) The strand is paired with its Watson–Crick complement and then exposed to hydroxyl radicals. The strand in the complex is then compared with the strand in the linear duplex. Previous studies have all revealed dramatic protection, relative to duplex, at the crossover points of immobile junctions. This protection is accentuated in double-crossover molecules, where conformational degrees of freedom are eliminated (Fu & Seeman, 1993). The characterization of the DAO molecule shows clear protection at the crossover points and at loci on the non-crossover strands about 4–5 nucleotides 3′ to the crossover; the non-crossover protection can be interpreted as resulting from the mutual occlusion of strands whose phasing brings them into proximity at this point (Churchill *et al.*, 1988; Kimball *et al.*, 1990; Fu & Seeman, 1993). Whereas we are using the same DAO complex that was previously studied, no further characterization has been undertaken.

Elsewhere, we have established the topology of DPONCC and have demonstrated that it is in fact the doubly linked catenane that it is designed to be (Fu *et al.*, 1994). Nevertheless, topology is not equivalent to structure, so we have done a hydroxyl radical autofootprinting analysis of DPONCC. The data in Figure 5 compare the cleavage in DPONCC and in the duplex molecules formed from its individual strands complexed with their Watson–Crick complements. Densitometer traces of the cleavage patterns are shown above and below a drawing of the molecule. The schematic contains triangles whose sizes correspond to the intensity of protection from hydroxyl radical cleavage. Three points are immediately apparent: (1) It is clear that the positions designed to be crossover points are indeed protected, relative to their duplex controls. (2) Dramatic protection is visible at the occluded sites between crossovers in the vicinity of residues 37 and 38; the sites near residues 78 and 79 are not accessible experimentally. In addition, occlusive protection one turn 5′ to these sites is visible on the distal arms on the left; the comparable sites on the other arms (ca. position 67) are beyond the limits of the experiment. (3) The $(dT)_4$ hairpin loops are also protected from hydroxyl radicals. The first two points demonstrate that DPONCC has the protection pattern expected from the designed double-crossover molecule.

Cleavage of DAO by Endonuclease VII. The endo VII cleavage pattern of DAO is shown in Figure 6. Figure 6a contains a schematic of the cutting pattern, and Figure 6b contains the autoradiogram of the gel from which the cutting

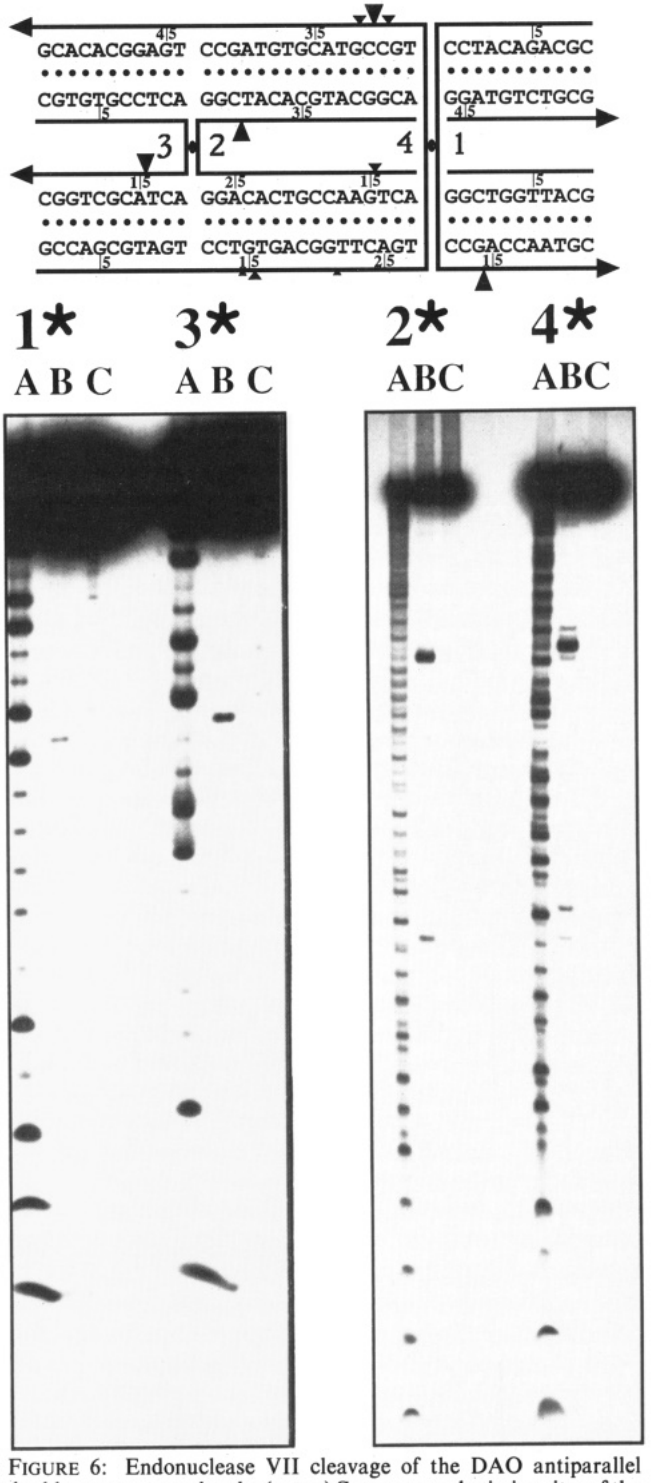

FIGURE 6: Endonuclease VII cleavage of the DAO antiparallel double-crossover molecule. (a, top) Sequence and scission sites of the DAO molecule. The molecule contains about 1.5 turns of DNA (16 nucleotide pairs on each domain) between the two crossover positions. The 3′ ends of the four strands are indicated by arrowheads. The strands are numbered at the center of the molecule. Note that the crossover on the left is formed by strands 2 and 3; the one on the right, by strands 1 and 4. The local backbone dyad axes are indicated by the lens-shaped figures in the middle of the crossovers. The scission sites are indicated by triangles; major sites are indicated by large triangles, and minor sites are indicated by small triangles. The nucleotide numbering from the 5′ ends is indicated for every tenth nucleotide, starting with the fifth one, for each strand. (b, bottom) Scission pattern of the DAO molecule. These are autoradiograms of denaturing gels. The panel on the left contains products from endo VII treatment in which the 22-nucleotide strands 1 and 3 are labeled, and the panel on the right contains the products of endo VII treatment in which the 54-nucleotide strands 2 and 4 are labeled. Lane A in each panel contains the Maxam–Gilbert (1980) A–G ladder of the strand, lane B contains the results of scission, and lane C is an untreated control. The major loci of scission are evident in lane B.

pattern has been determined. The short strands show scission only at a single position, 3 nucleotides 3′ to the crossover point, between nucleotides 14 and 15. This also corresponds to the primary point of scission on the long strands, between nucleotides 30 and 31. The primary cleavage site on strand 4 is flanked by two minor sites. The presence of multiple cleavage sites flanking a given locus has been noted previously with this enzyme (Mueller *et al.*, 1988; Kemper *et al.*, 1990). Minor cleavage sites may also be noted on the long strands 3 nucleotides 3′ to the junction in which they act as the helical strands. It should be noted that precautions are often required when studying the scissile activity of endo VII. In previous studies (Mueller *et al.*, 1988, 1990), we have used shamrock junctions to ensure that only resolution activities were being monitored, and not second cuts or nicking activities. Whereas it is not practical to take those measures with a DAO molecule, it is possible that we have detected a nicking activity with regard to the minor sites. The comparable sites are experimentally accessible in the short strands, but are not detected. A very weak cutting site 6 nucleotides 5′ to the crossover on strand 4 has not been reproduced in Figure 6b.

Cleavage of DPONCC by Endonuclease VII. The endo VII cleavage pattern of DPONCC is shown in Figure 7. Figure 7a contains a schematic of the cutting pattern, and Figure 7b contains the autoradiogram of the gel from which the cutting pattern has been derived. Although the derivation of Figure 6a from Figure 6b is straightforward, requiring only the interpretation of the ladder in the gel, the derivation of Figure 7a from Figure 7b is somewhat more oblique, because the strands are cyclic before endo VII treatment. Strand 1 is labeled in lanes 1–4 , and strand 2 is labeled in lanes 5–8, of Figure 7b. These lanes are interspersed with A–G sequencing ladders (Maxam & Gilbert, 1980). Lanes 1 and 5 are controls, containing the unrestricted linear 80-mer strand, 80-mer circles with slightly lower mobilities, and very slowly migrating catenanes at the tops of the lanes. These lanes also contain catenanes that have been restricted in their nominally unlabeled strand (*Rsa* cleavage of strand 2 in lane 1 and *Hha*I cleavage of strand 1 in lane 5). If any of this strand had happened to be labeled through some unforeseen circumstance, bands corresponding to linear molecules shorter than the 80-mers would be visible; none are, indicating that no cross-strand labeling has taken place.

Lane 2 contains the products of digesting strand 1 with *Nla*III. This is the most straightforward data, because the labeled phosphate is at the 5′ end of the restricted strand. Even though the fragments are greater than half the length of the molecule, the label is only contained in fragments whose length is measured in the 5′ → 3′ direction from the 5′ end. Two fragments (42 and 68 nucleotides long) are visible, corresponding to the major site shown in Figure 7a as **1** (between nucleotides 42 and 43) and the minor site shown in Figure 7a as **2** (between nucleotides 68 and 69). Exact positions of endo VII cleavage near the *Nla*III cleavage site are not readily accessible from restriction at that site, because they are too near the top of the lane or have run off the gel. Cleavage with *Taq*I produces a 43-nucleotide fragment (Figure 7b, lane 3), whose cutting site could be in either of two positions and still contain the label. This ambiguity is resolved in lane 4, showing cleavage with *Hha*I. Double cleavage with this enzyme shortens the strand by 16 nucleotides. The most prominent band is a doublet of strands 53 and 54 nucleotides long. The band corresponding to the 53-mer represents scission at position **1**. Therefore we conclude that we can use the band corresponding to the 54-mer to resolve the ambiguity about the position of the cleavage found in the *Taq*I digestion:

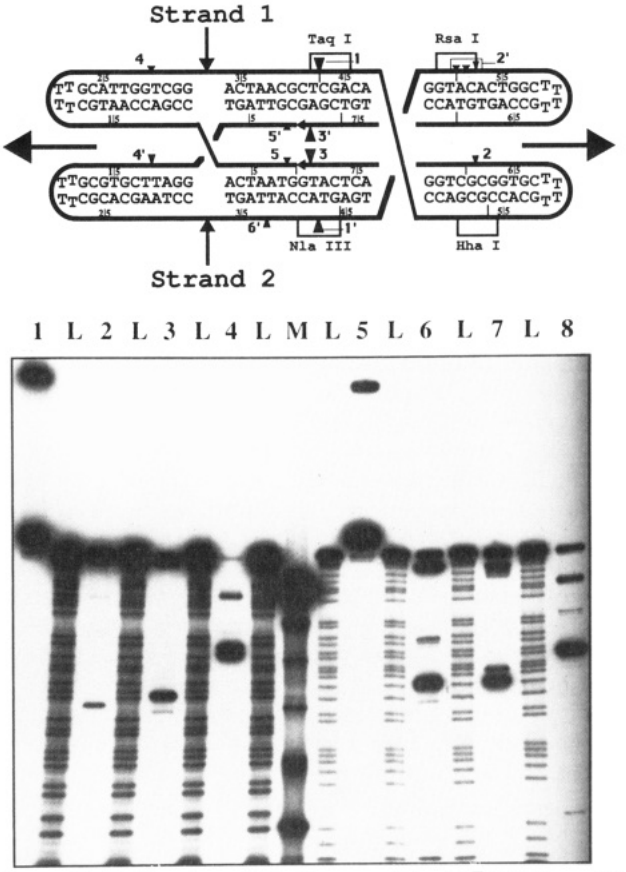

FIGURE 7: Endonuclease VII cleavage of the DPONCC parallel double-crossover catenane. (a, top) Restriction and endo VII scission sites of DPONCC. This panel summarizes the results of cleaving DPONCC with endonuclease VII. The sequences of the two strands are shown, and their 3′ ends are indicated by small arrowheads. The large arrows at either end of the drawing represent the possible molecular twofold symmetry axis that can relate the two backbones. The restriction recognition sites are shown as boxes outside the strands, and their scission points are drawn as thin lines inside the strands and perpendicular to them. The points of cleavage are indicated by triangles that represent their relative magnitudes. The sites on strand 1 are numbered 1–5, and those on strand 2 are numbered 1′–6′. When possible, the same number has been assigned to dyad-related sites (1–1′, 3–3′, and 5–5′). Sites 2 and 2′ or 4 and 4′ are not related by dyad symmetry. The strand numbering from the 5′ end of the preligation strands is indicated for every tenth nucleotide, starting with the fifth one, for both strands. (b, bottom) Scission pattern of DPONCC. This is an autoradiogram of a denaturing gel. The label is on strand 1 in lanes 1–4 and on strand 2 in lanes 5–8. Lanes labeled "L" contain the Maxam–Gilbert (1980) A–G ladder of the strand. The lane labeled "M" contains a series of linear length markers; the top one contains 70 nucleotides, followed by others containing 60, 50, 40, 30, and 20 nucleotides, respectively. Lanes 1 and 5 are controls containing, in order of increasing mobility, DPONCC catenane, uncleaved single 80-nucleotide circle, and 80-nucleotide linear strands. Some DPONCC in lane 1 has been restricted by *Rsa*I, and some DPONCC in lane 5 has been restricted by *Hha*I; the absence of bands corresponding to labeled linear molecules shorter than 80 nucleotides shows that there has been no cross-labeling of strands. Lanes 2–4 and 6–8 contain the products of digesting the 80-nucleotide linear fragment cleaved by endonuclease VII by restriction enzymes: lane 2, *Nla*III; lane 3, *Taq*I; lane 4, *Hha*I; lane 6, *Taq*I; lane 7, *Nla*III; lane 8, *Rsa*I.

Position **3** (between nucleotides 79 and 80) is the site of cleavage (Figure 7a). The faint band in lane 3 corresponds to site **5** (between nucleotides 1 and 2). There is another band in lane 4, containing a molecule about 16 nucleotides longer (69 or 70) than the prominent bands; whereas it is longer than fully restricted material, it may result from occasional single scissions by *Hha*I. Site **4** (between nucleotides 29 and 30), indicated in Figure 7a, is a very weak site of scission, visible on original gels but not reproduced in the photographs.

Analysis of cleavage on strand 2 is shown in lanes 5–8. The key restriction site, *Taq*I, is not exactly at the site of the label in strand 2, but is 4 nucleotides 5′ to it. We have prepared the sequencing ladders with strand 2 ligated and then restricted with *Taq*I, rather than using raw strand 2. There is ambiguity about the correlation of length with position in this molecule, but only for fragments containing eight or fewer nucleotides, which do not impinge on the interpretation of the data (lane 6). There is no ambiguity in the positions of endo VII cleavage for the major 46-nucleotide fragment, **1′** (between nucleotides 42 and 43), and the minor 56-nucleotide fragment, **2′** (between nucleotides 52 and 53; see Figure 7a). Two shorter and weaker sites, 55 and 54 nucleotides long, are associated with the 56-nucleotide band. The other strong cutting site produces a 77-nucleotide fragment at **3′** (between nucleotides 79 and 80). A faint band 41 nucleotides long (**6′**, between nucleotides 37 and 38) is seen 5 nucleotides 5′ to **1′**. Another minor fragment, 15 nucleotides long, corresponds to the position labeled **4′** (between nucleotides 18 and 19). Cleavage with *Nla*III (lane 7) permits analysis of parts of the strand inaccessible to *Taq*I. This lane contains a 45-mer band corresponding to **3′** and a 47-mer band corresponding to **4′**. The apparently thick band near the top of lane 7 (ca. 72–74 nucleotides long) is a poorly reproduced triplet of weaker cuts, similar to those produced by **2′** in lane 6; we ascribe them to the same site, although the intensities are reversed and position **6′** may contribute intensity to these bands. Lane 8 contains products of *Rsa*I cleavage. The thick band in lane 8 (51 or 52 nucleotides) corresponds to cleavage at both **1′** and **3′**. The weak band above it is about 61 or 62 nucleotides long, corresponding to the **2′** locus. The stronger band above it (71 or 72 nucleotides) derives from single nicking by *Rsa*I of a fragment cleaved at either **1′** or **3′**. A site is indicated as **5′** (between nucleotides 1 and 2) on strand 2; this is derived from a light band that is not reproduced in Figure 7b. Very weak sites, not visible on the gel reproductions in Figure 7b, correspond to cleavage of all the hairpin loops except the one on the upper right of DPONCC in Figure 7a; these loops are cleaved at either the 3′ or the 5′ end.

DISCUSSION

The Cleavage Sites on DAO Are the Same as Those in Molecules Containing a Single Branch Point. The major cutting sites in the DAO molecule, seen in Figure 6a, are those characteristic of cleavage by endo VII in immobile junctions containing a single branch point (Mueller *et al.*, 1988, 1990; Duckett *et al.*, 1988; Bhattacharyya *et al.*, 1991; Pottmeyer & Kemper, 1992). These sites are 3 nucleotides 3′ to the crossover point in each case, and they are twofold symmetric about the local structural pseudo-dyad axes associated with each branch point (Figure 6a). The site on strand 4 is flanked by minor sites, but the other sites are unusually specific. Cleavage in conventional (Duckett *et al.*, 1988; Pottmeyer & Kemper, 1992), shamrock (Mueller *et al.*, 1988, 1990), and tethered (Bhattacharyya *et al.*, 1991) junctions often reveals several adjacent sites of scission, but the double-crossover molecules are surprisingly clean. This may reflect the lack of conformational flexibility in these molecules. The few minor sites may represent secondary scission of previously cleaved molecules, from which the enzyme has not dissociated. Inspection of Figure 6a shows that we are well within the single-hit limit, but there is no evidence that endo VII dissociates from its substrate molecule without seeking other sites.

The Cleavage Sites on DPONCC Are Not the Same as Those in Molecules Containing a Single Branch Point. The four prominent cleavage sites are contained within the central portion of DPONCC, between the two crossovers, and they are symmetric across the molecular dyad between the parallel domains (horizontal in Figure 7a). However, these points of scission are not at the loci normally associated with endo VII resolution of Holliday junction analogs. These sites are on the crossover strands 5 nucleotides 5′ to the crossover on the right (**1** and **1′** in Figure 7a), and on the non-crossover strands 6 nucleotides 3′ to the crossover on the right (**3** and **3′** in Figure 7a). Positions **1** and **1′** on the crossover strands bear little structural or positional relationship to previous sites of cleavage associated with Holliday junction analogs. Whereas endo VII cleaves 3′ to unusual structures (Kemper *et al.*, 1990), it is useful to seek the recognition structure for these sites upstream from them. The closest available structure 5′ to sites **1** and **1′** is the interstrand contact point near residues 37 and 38 of each strand, 5 nucleotides away (Figure 5). Sites **3** and **3′** are 2 nucleotides 3′ to the interstrand contact point at residues 77 and 78.

One might argue that the normal sites of scission between crossovers in a parallel double-crossover are not sterically accessible. One of the advantages of using a DPON-type isomer, in contrast to a DPOW-type isomer (see Figure 3), is that those sites are not contained within the central portion of the molecule; they are in the distal arms, where there is likely to be somewhat more flexibility. Positions **2′** and **4′** roughly correspond to traditional endo VII cleavage sites, but the activity at those sites is much lower than that noted at **1′** and **3′**. Whereas endo VII is a packaging enzyme (Kemper & Garabett, 1981; Kemper *et al.*, 1981), the juxtaposition of intermolecular parallel backbones may represent a key substrate for its functional importance. Steric considerations derived from molecular model building (Seeman, 1988) suggest that the possible twofold symmetry axis of endo VII (Kosak & Kemper, 1990; Mueller *et al.*, 1990) is not aligned with the global molecular symmetry axis when DPONCC is cleaved.

Which Orientation Is the Natural Substrate of Endo VII Resolution? This is the first time that Holliday junction analogs constrained to be parallel or antiparallel, and treated with endo VII, have been compared. We detect no systematic sequence features associated with the major sites of scission; their symmetry in both cases suggests a structural basis for recognition. In agreement with previous work (Bhattacharyya *et al.*, 1991), we find that the products of the antiparallel junction are similar to those of unconstrained junctions. However, this is the first unambiguous demonstration that the endo VII cleavage products of parallel junctions differ from those of unconstrained junctions. We can conclude that endo VII does not change the structure of the unconstrained junction from antiparallel to parallel before cleaving it. The application of Occam's razor would lead to the conclusion that antiparallel Holliday junctions are indeed the substrates of endo VII. However, Crick (1988) has noted that this logical tool is not well suited to biological systems. In order to conclude that the antiparallel junction is the substrate within the cell, it is necessary to prove that the Holliday junction is unconstrained within the cell, just as the single Holliday junction is unconstrained in solution. At present, the state of the Holliday junction within the cell is unknown.

The finding that the parallel molecule is cleaved by endo VII shows that the issue of the natural substrate is not closed for this enzyme. The parallel molecule is an adequate substrate, and its cleavage is seen to be symmetrical. We have shown elsewhere that the parallel structure is not favored for molecules containing crossovers (Lu *et al.*, 1991; Fu &

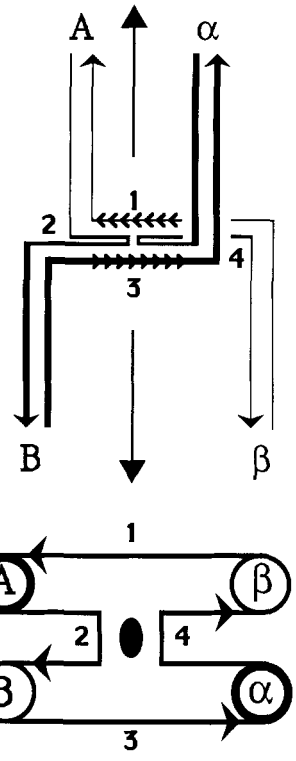

FIGURE 8: An antiparallel Holliday junction within a globally parallel context. Shown at the top is a view of a Holliday junction viewed somewhat obliquely to the dyad axis, which is represented by the two large vertical arrows. The four strands are numbered 1–4, counterclockwise around the crossover; their 3′ ends are indicated by arrowheads. The strands are drawn with different thicknesses in different sections to convey the idea of depth. Thus, strand 1 is entirely in the background, drawn as a thin line, and strand 3 is entirely in the foreground, drawn as a thick line. The 5′ end of strand 2 is in the background and is drawn as a thin line, but its 3′ end is in the foreground, and is drawn as a thick line; similarly, the 5′ end of strand 4 is in the foreground, drawn as a thick line, and its 3′ end is in the background, drawn as a thin line. Double-helical regions are represented by parallel lines. The allelic flanking markers **A** and α are shown at the top, and the allelic flanking markers **B** and β are at the bottom. There is a parallel arrangement between them. Nevertheless, the Holliday junction is locally antiparallel. This point is emphasized by the presence of a large number of arrowheads drawn along its non-crossover strands, 1 and 3. The right angles in the strands are an artistic device; these sharp kinks could be replaced by smooth curves. No lengths are specified in this drawing, but we imagine the scale to be large, tens to hundreds of nucleotides at least, to accommodate the stiffness of DNA. A view down the dyad axis of the same Holliday junction is shown at the bottom. Arrowheads indicate the 5′ → 3′ directions of the strands. The circles represent helices; those corresponding to **A** and α are drawn with thicker lines than those corresponding to **B** and β to indicate that they are nearer to the reader.

Seeman, 1993). However, we have also pointed out that in principle it could be stabilized by proteins or by distortions within a double-crossover context (Fu & Seeman, 1993). Were that to be the case within the cell, endo VII could act to resolve the junction, but it would generate different products from antiparallel resolution at the exact same branch point.

Locally Antiparallel Molecules Can Be Globally Parallel. The possibility that the Holliday junction may be antiparallel raises a potential problem for the interpretation of genetic data, which is often treated in terms of the parallel paradigm illustrated in Figure 2. In fact, it is not difficult to model the Holliday junction to be locally antiparallel, but within a larger parallel context (Seeman *et al.*, 1990). This point is illustrated in Figure 8. The top portion of this drawing is a slightly oblique view of the region flanking a Holliday junction. Our viewpoint is not perpendicular to the dyad, but has been raised sufficiently to enable visualizing some features of the Holliday junction in the center of the molecule. **A** and α represent allelic markers flanking the junction on one side, and **B** and β represent similar markers on the other side. The symmetry axis relates these markers, and it can be seen that the overall organization of the joined molecules is parallel, with the same connectivity shown in Figure 2. Nevertheless, the Holliday junction at the center has an antiparallel structure.

The crossover strands in Figure 8 are 2 and 4, and the helical strands are 1 and 3. In the central Holliday junction, strand 1 is antiparallel to strand 3, as emphasized by the arrowheads along those strands in the vicinity of the branch point. This is true despite the fact that the overall polarity of strand 1 is parallel to that of strand 3, and the overall polarity of strand 2 is parallel to that of strand 4. This figure has been drawn so that the helices containing **B** and α are closer to the reader, and those containing β and **A** are further from the reader. All of the DNA segments drawn are arbitrarily long; the right-angle bends are only an artistic device that can be replaced by smoothly curved double helices. The scale is arbitrary, but the drawing should be considered to have tens to hundreds of nucleotides per arm, in order to accommodate the known torsional stiffness of DNA [reviewed in Hagerman (1988)]. The bottom portion of Figure 8 is a view directly down the twofold axis of the same structure. Here, **A** and α are closer to the reader, and **B** and β are further away. It is clear that locally this is an antiparallel junction, with strands 1 and 3 having oppositely directed polarities.

It is important to realize that the antiparallel structure is a geometrical feature, not a topological feature. In principle, given enough flexibility, it could even arise in a double-crossover structure. Genetic experiments that are insensitive to the 3-D details of the Holliday structure in the vicinity of the crossover would not detect the antiparallel nature of the junction in Figure 8. If **A** and α were pulled upward and **B** and β were pulled downward, the bends would straighten, the domains flanking the crossover would rotate, and the junction would appear to be parallel; it would appear no different from the junctions in Figure 2, or the one on the right of Figure 1, except that it would have been rotated 90° about an axis vertical in the page.

The Cleavage Sites on DAO Suggest That Domain Rotation Is Not Required. The suggestion has been made recently that a 120° angle between the helical domains of the Holliday junction provides a recognition element for molecules that interact with Holliday junctions (Bhattacharyya *et al.*, 1991). The double-crossover molecules employed here provide an opportunity to test this suggestion. In particular, the DAO molecule has been characterized by hydroxyl radical footprinting, and the axes of its helical domains appear to be both coplanar and unbent (Fu & Seeman, 1993). Nevertheless, we find that the cleavage pattern of DAO is similar to that of unconstrained junctions. We do not know the structure of the enzyme-substrate complex, which might very well contain a bend. Nevertheless, such a bend would need to be induced by the enzyme, because it does not appear to be a feature of the DAO molecule.

ACKNOWLEDGMENT

We would like to thank Dr. John Mueller for performing preliminary experiments involving tethered junctions and for valuable discussions about that work. Drs. Richard Cunningham, Amy Kimball, and Thomas Tullius have also provided valuable insights.

REFERENCES

Bhattacharyya, A., Murchie, A. I. H., von Kitzing, E., Diekmann, S., Kemper, B., & Lilley, D. M. J. (1991) *J. Mol. Biol. 221*, 1191–1207.

Caruthers, M. H. (1985) *Science 230*, 281–285.

Chen, J.-H., Churchill, M. E. A., Tullius, T. D., Kallenbach, N. R., & Seeman, N. C. (1988) *Biochem*istry *27*, 6032–6038.

Churchill, M. E. A., Tullius, T. D., Kallenbach, N. R., & Seeman, N. C. (1988) *Proc. Natl. Acad. Sci. U.S.A. 85*, 4653–4656.

Cooper, J. P., & Hagerman, P. J. (1987) *J. Mol. Biol. 198*, 711–719.

Cooper, J. P, & Hagerman, P. J. (1989) *Proc. Natl. Acad. Sci. U.S.A. 86*, 7336–7340.

Crick, F. H. C. (1988) *What Mad Pursuit*, p 138, Basic Books, New York.

Dressler, D., & Potter, H. (1982) *Annu. Rev. Biochem. 51*, 727–761.

Du, S. M., Zhang, S., & Seeman, N. C. (1992) *Biochemistry 31*, 10955–10963.

Duckett, D. R., Murchie, A. I. H., Diekmann, S., Von Kitzing, E., Kemper, B., & Lilley, D. M. J. (1988) *Cell 55*, 79–89.

Eis, P. S., & Millar, D. P. (1993) *Biochemistry 32*, 13852–13860.

Fu, T.-J., & Seeman, N. C. (1993) *Biochemistry 32*, 3211–3220.

Fu, T.-J., Tse-Dinh, Y.-C., & Seeman, N. C. (1994) *J. Mol. Biol.* (in press).

Hagerman, P. J. (1988) *Annu. Rev. Biophys. Biophys. Chem. 17*, 265–286.

Hoess, R., Wierzbicki, A., & Abremski, K. (1987) *Proc. Natl. Acad. Sci. U.S.A. 84*, 6840–6844.

Holliday, R. (1964) *Genet. Res. 5*, 282–304.

Hsu, P. L., & Landy, A. (1984) *Nature (London) 311*, 721–726.

Jensch, F., & Kemper, B. (1986) *EMBO J. 5*, 181–189.

Johnson, R. D., & Symington, L. S. (1993) *J. Mol. Biol. 229*, 812–820.

Kallenbach, N. R., Ma, R.-I., & Seeman, N. C. (1983) *Nature (London) 305*, 829–831.

Kemper, B., & Brown, D. T. (1976) *J. Virol. 18*, 1000–1015.

Kemper, B., & Janz, E. (1976) *J. Virol. 18*, 992–999.

Kemper, B., & Garabett, M. (1981) *Eur. J. Biochem. 115*, 123–131.

Kemper, B., Garabett, M., & Courage, U. (1981) *Eur. J. Biochem. 115*, 133–141.

Kemper, B., Pottmeyer, S., Solaro, P., & Kosak, H. (1990) in *Structure and Methods* (Sarma, R. H., Sarma, M. H., Eds.) Vol. I, pp 215–229, Adenine Press, New York.

Kim, J. S., Sharp, P., & Davidson, N. (1972) *Proc. Natl. Acad. Sci. U.S.A. 69*, 1948–1952.

Kimball, A., Guo, Q., Lu, M., Kallenbach, N. R., Cunningham, R. P., Seeman, N. C., & Tullius, T. D. (1990) *J. Biol. Chem. 265*, 6544–6547.

Kitts, P. A., & Nash, H. A. (1987) *Nature (London) 329*, 346–348.

Kleff, S., & Kemper, B. (1988) *EMBO J. 7*, 1527–1535.

Kosak, H., & Kemper, B. (1990) *Eur. J. Biochem. 194*, 779–784.

Lilley, D. M. J., & Kemper, B. (1984) *Cell 36*, 413–422.

Lilley, D. M. J., & Clegg, R. M. (1993) *Annu. Rev. Biophys. Biomol. Struct. 22*, 299–328.

Lloyd, R. G., & Sharples, G. J. (1993) *EMBO J. 12*, 17–22.

Lu, M., Guo, Q., Mueller, J. E., Kemper, B., Studier, F. W., Seeman, N. C., & Kallenbach, N. R. (1990) *J. Biol. Chem. 265*, 16778–16785.

Lu, M., Guo, Q., Seeman, N. C., & Kallenbach, N. R. (1991) *J. Mol. Biol. 221*, 1419–1432.

Maxam, A. M., & Gilbert, W. (1980) *Methods Enzymol. 65*, 499–560.

Mizuuchi, K., Kemper, B., Hays, J., & Weisberg, R. (1982) *Cell 29*, 347–365.

Mueller, J. E. (1991) Ph.D. Thesis, State University of New York, Albany, NY.

Mueller, J. E., Kemper, B., Cunningham, R. P., Kallenbach, N. R., & Seeman, N. C. (1988) *Proc. Natl. Acad. Sci. U.S.A. 85*, 9441–9445.

Mueller, J. E., Newton, C. J., Jensch, F., Kemper, B., Cunningham, R. P., Kallenbach, N. R., & Seeman, N. C. (1990) *J. Biol. Chem. 265*, 13918–13924.

Murchie, A. I. H., Clegg, R. M., von Kitzing, E., Duckett, D. R., Diekmann, S., & Lilley, D. M. J. (1989) *Nature (London) 341*, 763–766.

Nunes-Duby, S. E., Matsumoto, L., & Landy, A. (1987) *Cell 50*, 779–788.

Panyutin, I. G., & Hsieh, P. (1993) *J. Mol. Biol. 230*, 413–424.

Pottmeyer, S., & Kemper, B. (1992) *J. Mol. Biol. 223*, 607–615.

Seeman, N. C. (1982) *J. Theor. Biol. 99*, 237–247.

Seeman, N. C. (1988) *J. Biomol. Struct. & Dyn 5*, 997–1004.

Seeman, N. C. (1990) *J. Biomol. Struct. & Dyn. 8*, 573–581.

Seeman, N. C., & Kallenbach, N. R. (1994) *Annu. Rev. Biophys. Biomol. Struct. 23*, 53–86.

Seeman, N. C., Mueller, J. E., Chen, J.-H., Churchill, M. E. A., Kimball, A., Tullius, T. D., Kemper, B., Cunningham, R. P., & Kallenbach, N. R. (1990) in *Structure and Methods* (Sarma, R. H., & Sarma, M. H., Eds.) Vol. I, pp 137-156, Adenine Press, New York.

Thompson, B. J., Camien, M. N., & Warner, R. C. (1976) *Proc. Natl. Acad. Sci. U.S.A. 73*, 2299–2303.

Tsaneva, I. R., Müller, B., & West, S. C. (1992) *Cell 69*, 1171–1180.

Tullius, T. D., & Dombroski, B. A. (1985) *Science 230*, 679–681.

Wang, Y., Muller, J. E., Kemper, B., & Seeman, N. C. (1991) *Biochemistry 30*, 5667–5674.

West, S. C. (1992) *Annu. Rev. Biochem. 61*, 603–640.

Zhang, S., Fu, T.-J., & Seeman, N. C. (1993) *Biochemistry 32*, 8062–8067.